DEPARTMENT OF COMPUTER SCIENCE
UNIVERSITY OF COPENHAGEN

Multiphase Local Mean Geodesic Active Regions

Jacob Daniel Kirstejn Hansen, François Bernard Lauze
{jdkh, francois}@di.ku.dk

Summary

We present two similar variational methods for multiphase segmentation of complex weakly structured 3D images affected by local and global intensity inhomogeneities as is observed in micro-tomography. The methods use a fixed number of classes and utilize local image averages as region descriptors to produce per voxel posterior probabilities a la Hidden Markov Measure Field Models (HMMFM). The methods use a weighted Total Variation (wTV) and weighted Dirichlet (squared gradient) as regularizers respectively.

Our problem

We aim to segment X-ray computerised micro and nanotomograph samples of geological origin. Samples contain homogeneous materials with flat surfaces and edges, but their shapes are rather complex and not well-structured. We model images with these properties as a function $u : \mathbb{R}^d \to \mathbb{R}$, with $d = 2, 3$

$$u = L\left(\sum_{i=1}^{n} \alpha \chi_{\Omega_i}\right) + \eta \tag{1}$$

where Ω_i is the ith individual segment and α_i its intensity. L models blur and partial volume effects. η represents additive bias field and noise, which is considered Gaussian in high-photon-count synchrotron imaging. Figure 1 shows an example of an experimental dataset with local bias fields.

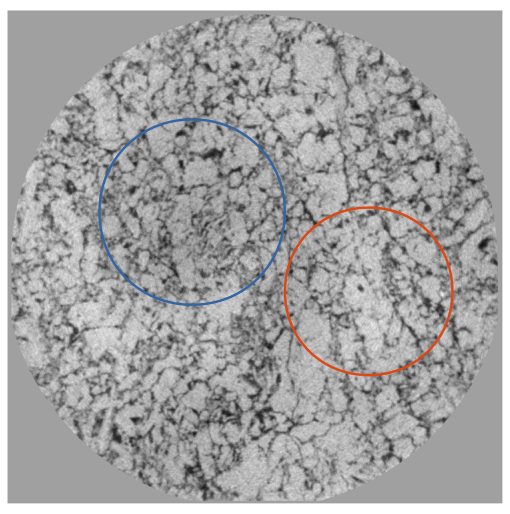

Figure 1: Experimental dataset with highlighted intensity imhomogeneity areas with highlighted intensity imhomogeneity areas.

Our approach

- As in our previous work, we use a local mean estimate in the data fidelity term to account for observed intensity inhomogeneities.
- The smoothing kernels can be any rotationally symmetric kernel, but we have used Gaussian and moving average kernels, of supervised extent (standard deviation and radius), based on the variation degree of the unknown bias field.
- To accomodate uncertainty in label estimates, we use a soft labelling approach, formalized by HMMFM. Additionally, to deal with partial volume effects at segment interfaces, we propose to use a Tikhonov regularization on the label field. Otherwise we use TV regularization.
- To avoid oversmoothing strong edges, we propose to locally weigh the regularization by any chosen constant function, depending on the image.

Model overview

Our proposed energy formulations are

$$\begin{aligned}\mathcal{E}_{wTV}(\mathbf{c},\mathbf{v}) &= \frac{1}{2}\sum_{i=1}^{n}\int_\Omega g * \left[(u - c_i(\boldsymbol{x}))^2 \mathbf{v}_i\right](\boldsymbol{x})\, d\boldsymbol{x} + \mu \mathcal{J}_h(\mathbf{v}),\\ \mathcal{E}_{wQ}(\mathbf{c},\mathbf{v}) &= \frac{1}{2}\sum_{i=1}^{n}\int_\Omega g * \left[(u - c_i(\boldsymbol{x}))^2 \mathbf{v}_i\right](\boldsymbol{x})\, d\boldsymbol{x} + \frac{\mu}{2}||D\mathbf{v}||_h^2\\ \mathbf{v} &\in \Sigma_n(a.e.)\end{aligned}$$

with Σ_n being the standard simplex, $||D\mathbf{v}||_h^2 = \sum_{i=1}^{n}\int_\Omega h|D\mathbf{v}|^2$, and $\mathcal{J}_h$ given as

$$\mathcal{J}_h(\mathbf{v}) = \begin{cases}\int_\Omega \psi^{**}(x, D\mathbf{v}) & \mathbf{v} \in BV_h(\Omega, \Sigma_n)\\ +\infty & \mathbf{v} \notin BV_n(\Omega, \Sigma_n),\end{cases}$$

where ψ^{**} is the convex relaxation w.r.t. $\boldsymbol{p} \in \mathbb{R}^{n\times d}$ in

$$\psi(\boldsymbol{x}, \boldsymbol{p}) = \begin{cases} h(\boldsymbol{x})|p| & if\, \boldsymbol{p} = (e_i - e_j)\otimes p\\ +\infty & otherwise.\end{cases} \tag{2}$$

and $BV_h(\Omega, \Sigma_n) = \{\mathbf{v} : \Omega \leftarrow \Sigma_n, v_i \in BV_h(\Omega)\}$, $BV_h(\Omega)$ being the space of *weighted total variation* of u, $\boldsymbol{J}_h(u) = \int_\Omega h|Du|$, the latter given as

$$\boldsymbol{J}(u) = \inf\left\{\int_\Omega u \operatorname{div}\phi\, d\boldsymbol{x}, \phi \in \mathcal{C}_c^1(\Omega, \mathbb{R}^d), ||\phi(x)|| \le h(x)\right\} \tag{3}$$

Algorithm and optimization

We use an alternate approach for optimizing the two energy formulations for $\mathbf{c}$ and $\mathbf{v}$, which is outlined in Algorithm 1.

Algorithm 1: Sketch of the algorithms.
Input: Input image volume u, number of classes n, weight parameter μ, kernel g and maximum number of iterations L_{RS}.
Output: Segmentation $(\mathbf{v}, \mathbf{c})$ of u .
Initialisation: Run a K-means or Otsu clustering to produce $(\mathbf{c}^0, \mathbf{v}^0)$ from u. For $\mathcal{E}_{wTV}$, an extra variable $\bar{\mathbf{v}}^0$ is initialised as $\mathbf{v}^0$ and dual variable $\boldsymbol{\xi}$ is initialised as 0, see below.
for $r = 0$ to L_{RS} **do**
Solve for $\mathbf{c}^{r+1}$ from u and $\mathbf{v}^r$.
Solve for $\mathbf{v}^{r+1}$ from u and $\mathbf{c}^{r+1}$.
end for

The updates on $\mathbf{c}$ are computed from

$$c_i(\mathbf{x}) = \frac{(u\mathbf{v}_i) * g(\mathbf{x})}{\mathbf{v}_i * g(\mathbf{x})}, \quad \mathbf{x} \in \operatorname{supp} \mathbf{v}_i. \tag{4}$$

For updates on the HMMFM variable $\mathbf{v}$ for $\mathcal{E}_{wTV}$ we use the framework of Chambolle, Cremers, and Pock (a convex approach to minimal partitions, 2011), modified to include our weight function h.

$$\begin{aligned}\mathcal{E}_{i+1}^r &= \mathcal{P}_{K_h}\left(\mathcal{E}_i^r + \tau_r \nabla \bar{\mathbf{v}}_i^r\right)\\ \mathbf{v}_{i+1}^r &= \mathcal{P}_{\mathcal{L}_n}\left(\mathbf{v}_i^r + t_r\left(div\mathcal{E}_{i+1}^r - \nabla_\mathbf{v}\mathcal{E}_D\right)\right)\\ \bar{\mathbf{v}}_{i+1}^r &= 2\mathbf{v}_{i+1}^r - \mathbf{v}_i^r,\end{aligned}$$

where $\mathcal{P}_{K_h}$ is the orthogonal projection onto the set $K_h = \left\{\mathcal{E} \in \mathcal{C}_c^1(\Omega, \mathbb{R}^{n\times d}), \mathcal{E}(\boldsymbol{x}) \in K_{h(x)}, \forall \mathbf{x} \in \Omega\right\}$, with $K_\alpha = \{\mathbf{q} = (q_i, \dots, q_n)^T \in \mathbb{R}^{n\times d} : |q_i - q_j \le \alpha, \forall i < j|\}$ and $\mathcal{P}_{\mathcal{L}_n}$ orthogonally projects to the standard simplex. A simple proximal method is used for $\mathcal{E}_{wQ}$ and its gradient is given by

$$\nabla_\mathbf{v}\mathcal{E}_{wQ} = \nabla_\mathbf{v}\mathcal{E}_D - \mu\nabla\cdot(hD\mathbf{v}) \tag{5}$$

$\mathcal{E}_D$ is here the shared data term of our two energy functions and $\nabla\cdot$ the vector divergence operator. The implicit descent step therefore becomes $\overline{\mathbf{v}^r} = \mathbf{v}^r - t_r\left(\nabla_\mathbf{v}\mathcal{E}_{wQ} - \nu\nabla\cdot\left(h\nabla\overline{\mathbf{v}^r}\right)\right)$, i.e. we solve the following equation

$$\left(-\nu\nabla\cdot h\nabla + t_r^{-1}id\right)\overline{\mathbf{v}^{r+1}} = t_r^{-1}\mathbf{v}_r - \nabla_\mathbf{v}\mathcal{E}_D. \tag{6}$$

In the following we set the structure function as

$$h(\mathbf{x}) = \frac{1}{1 + \left(\frac{|\nabla(g_\sigma * u)|}{\kappa}\right)^2} \tag{7}$$

Experimental validation

We evaluate results on a synthetic volume consisting of randomly distributied balls in a volume of size 250^3, with noise and bias fields, expecting 4 segments.

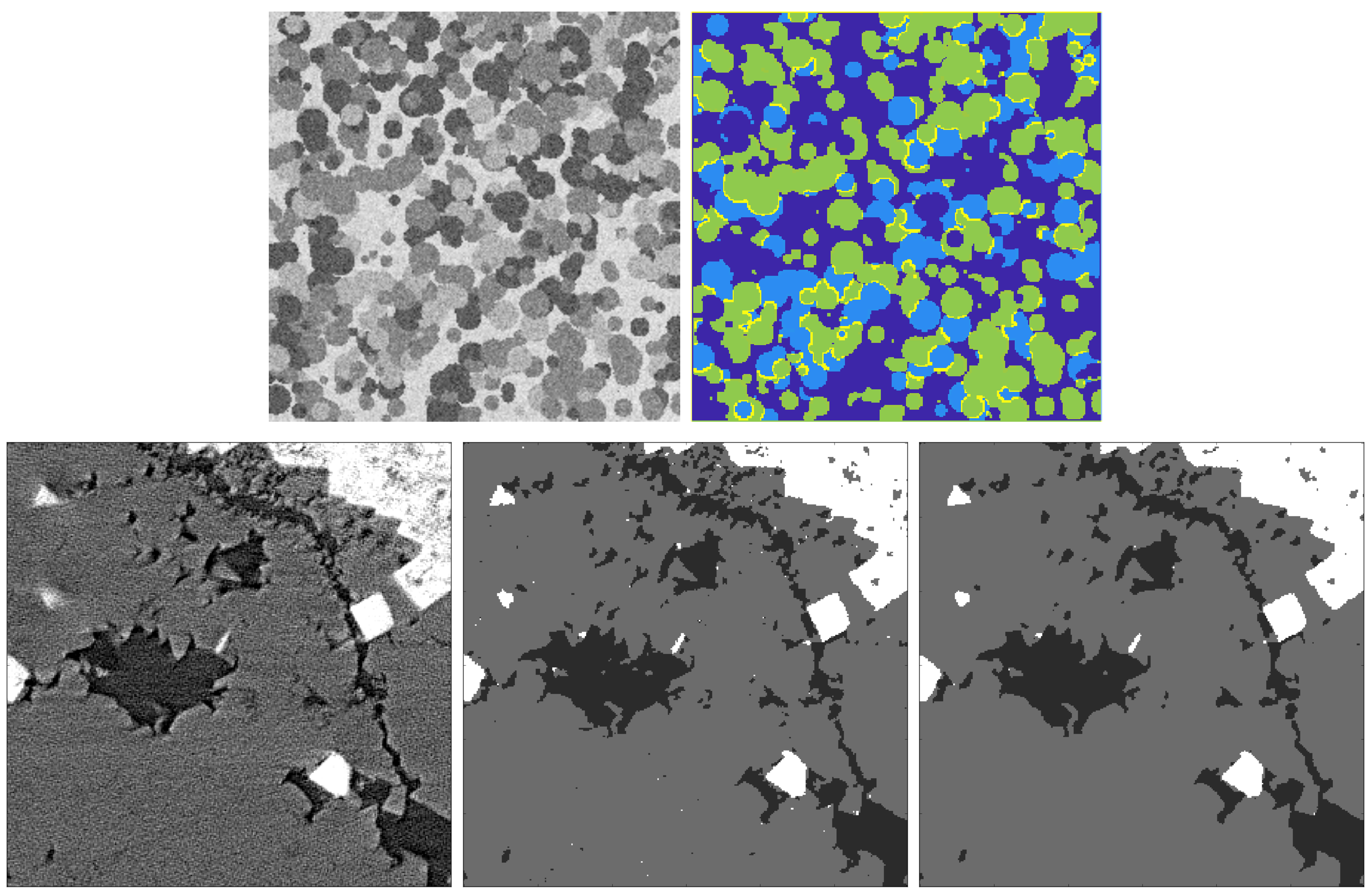

Figure 2: Row 1: Synthetic data and segmentation. Row 2: Experimental data, $\mathcal{E}_{wQ}$, and $\mathcal{E}_Q$ segmentations respectively.

Quality measures

We report Dice score index, true positive rate (TPR), true negative rate (TNR), and positive predictive value (PPV). We compare with our previous unweighted work using nearest neighbour kernels, as they slightly outperformed Gaussian kernels. We also compare with the regular piecewise constant Mumford-Shah, Otsu's thresholding method and a dual filtering approach, that utilizes an unsharp mask and median filter before threshoding, that is popular in geosciences.

Table 1: DSC, TPR, TNR, and PPV values for the segmentation results of the synthetic volume, using the selected methods.

Method	kernel	DSC	TPR	TNR	PPV
Tikhonov	NN	0.989286	0.97406	0.99336	0.98296
TV	NN	0.984218	0.96703	0.98956	0.97013
W-Tikhonov	NN	**0.990615**	**0.97918**	**0.99376**	**0.98325**
W-TV	NN	0.980704	0.92985	0.97880	0.94153
Method	**-**	**DSC**	**TPR**	**TNR**	**PPV**
PCMS	-	0.958090	0.88087	0.98259	0.94811
Otsu	-	0.894342	0.78868	0.93196	0.80911
Dual filter	-	0.954899	0.90980	0.96833	0.91485